Journal of Cranio-Maxillo-Facial Surgery 52 (2024) 48–54

Contents lists available at ScienceDirect

Journal of Cranio-Maxillo-Facial Surgery

journal homepage: www.jcmfs.com

Automated three-dimensional analysis of facial asymmetry in patients with syndromic coronal synostosis: A retrospective study

Tsun Man Choi [a,*,1], Xianjing Liu [a,b,1], Tareq Abdel-Alim [b,c], Marie-Lise van Veelen [c], Irene Margreet Jacqueline Mathijssen [d], Eppo Bonne Wolvius [a], Gennady Vasilievich Roshchupkin [b,e]

[a] Erasmus Medical Centre, Department of Oral Maxillofacial Surgery, Special Dental Care and Orthodontics, Dutch Craniofacial Centre, Rotterdam, the Netherlands
[b] Erasmus Medical Centre, Department of Radiology and Nuclear Medicine, Rotterdam, the Netherlands
[c] Erasmus Medical Centre, Department of Neurosurgery, Dutch Craniofacial Centre, Rotterdam, the Netherlands
[d] Erasmus Medical Centre, Department of Plastic and Reconstructive Surgery and Hand Surgery, Dutch Craniofacial Centre, Rotterdam, the Netherlands
[e] Erasmus Medical Centre, Department of Epidemiology, Rotterdam, the Netherlands

ARTICLE INFO

Handling Editor: Prof. Emeka Nkenke

Keywords:
Craniosynostoses
Facial asymmetry
Photogrammetry
Craniofacial abnormalities
Congenital abnormalities
Three-dimensional imaging

ABSTRACT

Craniosynostosis, characterized by premature fusion of one or more cranial sutures, results in a distorted skull shape. Only three studies have assessed facial asymmetry manually in unicoronal synostosis patients. It is therefore important to understand how uni- and bicoronal synostosis affect facial asymmetry with a minimum risk of human bias.

An automated algorithm was developed to quantify facial asymmetry from three-dimensional images, generating a mean facial asymmetry (MFA) value in millimeters to reflect the degree of asymmetry. The framework was applied to analyze postoperative 3D images of syndromic patients ($N = 35$) diagnosed with Muenke syndrome, Saethre-Chotzen syndrome, and *TCF12*-related craniosynostosis with respect to MFA values from a healthy control group ($N = 89$).

Patients demonstrated substantially higher MFA values than controls: Muenke syndrome (unicoronal 1.74 ± 0.40 mm, bicoronal 0.77 ± 0.21 mm), Saethre-Chotzen syndrome (unicoronal 1.15 ± 0.20 mm, bicoronal 0.69 ± 0.16 mm), and *TCF12*-related craniosynostosis (unicoronal 1.40 ± 0.51 mm, bicoronal 0.66 ± 0.05 mm), compared with controls (0.49 ± 0.12 mm). Longitudinal analysis identified an increasing MFA trend in unicoronal synostosis patients.

Our study revealed higher MFA in syndromic patients with uni- and bicoronal synostosis compared with controls, with the most pronounced MFA in Muenke syndrome patients with unilateral synostosis. Bicoronal synostosis patients demonstrated higher facial asymmetry than expected given the condition's symmetrical presentation.

1. Introduction

Craniosynostosis is a condition characterized by the premature fusion of one or more cranial sutures, leading to restricted skull growth in the direction perpendicular to the premature fused suture (Virchow, 1851). This condition can manifest as non-syndromic craniosynostosis, where it occurs in isolation, or as syndromic craniosynostosis, where it is associated with other anomalies that form clinically recognized syndromes, typically part of a genetic condition. The latter includes, among others, Muenke syndrome, Saethre-Chotzen syndrome, and *TCF12*-related craniosynostosis (Saethre, 1931; Chotzen, 1932; Bellus et al., 1996; El Ghouzzi et al., 1997, 1999; Howard et al., 1997; Muenke et al., 1997). *The prevalence of Muenke syndrome is* approximately 1:96 000 among newborns, compared with approximately 1:105 000 for Saethre-Chotzen syndrome, and approximately 1:210 000 for *TCF12*-related craniosynostosis (Cornelissen et al., 2016).

* Corresponding author. Erasmus Medical Centre, Department of Oral Maxillofacial Surgery, Special Dental Care and Orthodontics, Dutch Craniofacial Centre, PO Box 2040, 3000 CA, Rotterdam, the Netherlands.
E-mail address: t.choi@erasmusmc.nl (T.M. Choi).
[1] These authors contributed equally to this work.

https://doi.org/10.1016/j.jcms.2023.11.006
Received 21 August 2023; Accepted 23 November 2023
Available online 29 November 2023

Patients with syndromic craniosynostosis usually undergo surgical treatment to correct functional problems, such as inhibited skull growth, breathing problems, exorbitism, and malocclusion (Hohoff et al., 2007; Den Ottelander et al., 2019; De Goederen et al., 2021). In addition to these functional problems, surgery also aims to harmonize proportions and correct excessive facial asymmetries. Facial asymmetry is not exclusive to craniosynostosis patients, as it is also present in the healthy population (Ferrario et al., 1993; Ercan et al., 2008). However, more severe facial asymmetry has been observed in 90% of unicoronal craniosynostosis patients compared with a healthy control group (Öwall et al., 2016).

Facial asymmetry has also been reported in craniosynostosis syndromes with involvement of one or both coronal sutures (Gallagher et al., 2003; Doherty et al., 2007). Only three studies have assessed facial asymmetry in unicoronal synostosis patients using photogrammetry. However, asymmetry was assessed manually in these studies (Cornelissen et al., 2013; Öwall et al., 2016, 2019). It is therefore important to understand how both uni- and bicoronal synostosis affect facial asymmetry with a minimum risk of human bias.

In order to effectively and objectively quantify the differences in facial asymmetry between patients with unicoronal and bicoronal synostosis over time, it is important to develop an automated tool that can accurately measure these variations in a three-dimensional context, and which incorporates a quantitative metric that represents the severity of facial asymmetry. To automate the process, a standardized and objective pipeline is required, reducing the potential for human error or bias.

The objective of this study was to develop and apply an automated method to quantitatively and objectively measure facial asymmetry in postoperative 3D images of patients with Muenke syndrome, Saethre-Chotzen syndrome, and *TCF12*-related craniosynostosis in whom one or both coronal sutures were affected, and to correlate the results with those for a Dutch control group. Furthermore, the aim of this study was to conduct a longitudinal analysis of facial asymmetry in these three syndromes, specifically examining the development of facial asymmetry in unicoronal and bicoronal craniosynostosis over time.

2. Materials and methods

A search was conducted for available 3D images for patients who were referred between 2005 and 2022 to the craniofacial team at Sophia Children's Hospital Rotterdam in the Netherlands. All included patients were clinically diagnosed by an expert (e.g. a clinical geneticist or a craniofacial plastic surgeon) with Muenke syndrome (P250R mutation in *FGFR3*), Saethre-Chotzen syndrome (mutations or rearrangements in *TWIST1*), or *TCF12*-related craniosynostosis syndrome (mutations or rearrangements in *TCF12)*. The medical records of the patients were checked for available 3D images:

All patients with 3D images were selected for inclusion according to the following criteria: diagnosis molecularly confirmed; were of Caucasian descent; had only premature fusion of left and/or right coronal suture(s); had undergone only one craniofacial surgery; were younger than 18 years; had undergone no orthodontic treatment; had no extraction of permanent teeth; and had not undergone maxillary osteotomy. Patients were excluded for the following reasons: diagnosis was not molecularly confirmed; were not of Caucasian descent; had premature fusion of any other suture besides the coronal; had not undergone only one craniofacial surgery; were older than 18 years old at the time of the 3D image; had undergone orthodontic treatment; had extraction of permanent teeth or had undergone a maxillary osteotomy. Based on the inclusion criteria, 101 patients were eligible.

In addition, in order to examine how facial asymmetry developed over time after surgery, facial images of these patients were used that had been collected at different time points.

This retrospective cross-sectional study was approved by the Medical Ethics Committee of the Erasmus University Medical Centre in Rotterdam, the Netherlands (MEC-2013-536). The images, made using three-dimensional photogrammetry, were obtained as part of orthodontic documentation according to the treatment protocol used by the craniofacial team in the Erasmus University Medical Centre Rotterdam, the Netherlands.

The control group comprised children from the Generation R Study, an ongoing population-based cohort study of pregnant women and their children from fetal life onwards (Jaddoe et al., 2006). All women living in the study area of Rotterdam, the Netherlands, who delivered between April 2002 and January 2006, were eligible.

2.1. Three-dimensional image acquisition and preprocessing

Three-dimensional images were captured by a trained photographer in a designated 3D imaging room without windows that had a consistent amount of ambient lighting. The distance and angle between the patient and cameras were fixed when taking pictures, as described by the manufacturer's guidelines. The system (3dMDfacial System; 3dMD Ltd., Atlanta, GA, USA), which was calibrated daily, captures images in 1.5 ms using a 2-pod configuration tailored for frontal facial image acquisition, which includes both ears. Each three-dimensional image comprises approximately 20 000 points, and the texture map is of eight megapixels. All images of patients were standardized. During image capturing, all patients maintained a neutral facial expression with open eyes and relaxed, opposed lips. Patients were sitting on an adjustable chair, which was used in a fixed position to assure a standard level of height and fixed distance between the subject and the camera system.

The captured images covered the facial region from the ears to the medial facial area, and from the hairline to the menton, and were free from imaging artifacts. To ensure images of sufficient quality for further analysis, the photographer immediately visually assessed the quality of the captured images post-acquisition to confirm the completeness of three-dimensional image data.

The selected three-dimensional images were exported from the 3dMDpatient 4.0 software as polygon files (.ply) with textures. Subsequently, a three-dimensional morphology registration pipeline was adopted (Booth et al., 2018) to build the three-dimensional images into a template-based dataset. In this dataset, each facial image was represented by a three-dimensional mesh, with a consistent vertex number and edge connectivity.

2.2. Algorithm for facial asymmetry measurement

An automatic framework was developed for the evaluation of facial asymmetry using three-dimensional photogrammetry (Fig. 1). The process began by taking the facial shape of each subject as input, after which a mirrored reflection was generated. This mirrored image was then automatically aligned with the input via rigid registration. The vertex-wise distance between these two aligned facial shapes was then computed. Finally, two quantitative outcomes were produced for each subject: 1) a facial heatmap based on the distance where zero-error regions were perfectly symmetric while higher-error regions were more asymmetric; 2) a mean facial asymmetry (MFA) based on the mean of the error:

$$\mathrm{MFA}=\frac{\sum_{i}^{N_{vertex}/2}\sqrt[2]{(x_i-x_i^{'})^2+(y_i-y_i^{'})^2+(z_i-z_i^{'})^2}}{N_{vertex/2}}\ (\mathrm{mm}) \quad (1)$$

where N_{vertex} is the number of vertices in a facial shape, $[x_i, y_i, z_i]$ is the vertex of the input facial shape, and $[x_i^{'}, y_i^{'}, z_i^{'}]$ is the vertex in the mirrored image closest to $[x_i, y_i, z_i]$. The unit of MFA is mm.

Furthermore, as shown in the facial heatmap (Fig. 1), the face was further segmented into three parts: upper face segment (hairline to glabella), mid face segment (glabella to subnasale), and lower face segment (subnasale to menton). Therefore, the MFA was computed for each segment. To implement the segmentation, facial landmarks were

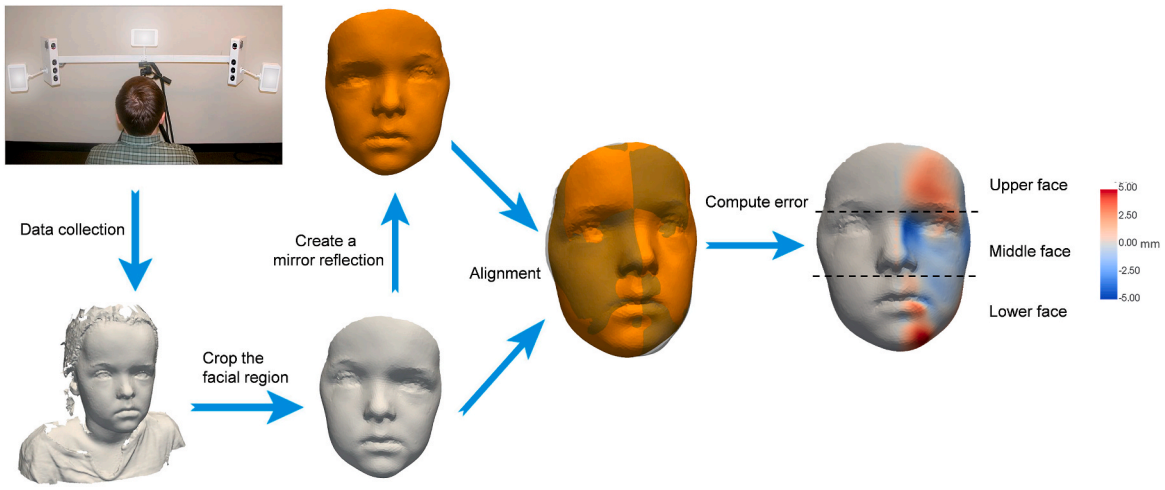

Fig. 1. Developed pipeline for facial asymmetry measurement. The colored half of the face represents asymmetrical features (red: expanding outward with respect to the contralateral half).

first automatically detected. Then the face was automatically divided into three segments based on these facial landmarks.

The developed framework was applied to study facial asymmetry in patients diagnosed with Muenke syndrome, Saethre-Chotzen syndrome, and *TCF12*-related craniosynostosis syndrome, as well as in control subjects. Asymmetry metrics obtained from the control group served as a baseline to help interpret the extent of facial asymmetry within the studied patient populations.

2.3. Statistical analysis

A linear regression analysis was performed to evaluate whether there was a significant difference in MFA between patients and controls. In this model, MFA served as the dependent variable, while the presence (or absence) of craniosynostosis, age, and gender functioned as independent variables. A *p*-value below 0.05 was considered statistically significant.

The patients were first divided into unicoronal and bicoronal craniosynostosis subgroups. Further stratification within each subgroup was then carried out based on two factors: 1) the three craniosynostosis syndromes (Muenke syndrome, Saethre-Chotzen syndrome, and *TCF12*-related craniosynostosis syndrome); and 2) the three horizontal segments of the face — upper face segment (hairline to glabella), mid face segment (glabella to subnasale), and lower face segment (subnasale to menton). In addition, a longitudinal analysis was conducted on subjects whose facial images were available at different time points, with the aim of investigating how MFA changed over time. The average slope was calculated for unicoronal and bicoronal synostosis subgroups and controls as:

$$Slope = \frac{MFA^{T2} - MFA^{T1}}{T2 - T1} \ (\text{mm / year})$$

where T_1 and T_2 are the subsequent timepoints at which 3D photos were acquired.

2.4. Implementation details

The algorithm for facial asymmetry measurement was constructed using the Python programming language. The facial landmarks were located via an open-source library (https://github.com/LightOfMonet/3Dface_landmark). The rigid registration algorithm originated from the Matlab method 'pcregistericp' (https://nl.mathworks.com/help/vision/ref/pcregistericp.html). The dense error (or distance) was calculated with the 'menpo3d' Python package using the 'VTKClosestPointLocator' (Alabort-i-Medina et al., 2014). This algorithm locates the vertex in the mirrored image closest to a given input vertex in the source facial shape. By processing each vertex, a dense error map was generated.

The statistical analysis was performed using the 'statsmodels' Python package (Seabold et al., 2010.)

3. Results

3.1. Patient characteristics

In total, 66 patients were excluded because the inclusion criteria were not met. After excluding these patients, 35 patients were eligible for inclusion (Fig. 2).

The final study group consisted of 35 patients with a mean age of 10.6 years (SD 3.18) at the time of inclusion — 24 females (mean age 10.6; SD 3.26) and 11 males (mean age 10.5; SD 3.16). Of this sample, 16 patients had unicoronal craniosynostosis, of which seven had Muenke syndrome, four had Saethre-Chotzen syndrome. Five patients had *TCF12*-related craniosynostosis and 19 patients had bicoronal craniosynostosis, of which 11 had Muenke syndrome, four had Saethre-Chotzen syndrome, and four had *TCF12*-related craniosynostosis (Table 1). 18 patients had Muenke syndrome, with a mean age of 11.2 (SD 2.88), eight patients had Saethre-Chotzen syndrome, with a mean age of 8.4 (SD 3.12), and nine patients had *TCF12*, with a mean age of 11.2 (SD 3.29).

For the longitudinal analysis, patients were selected with multiple 3D images that were in the same study population as mentioned previously, and as described in Table 1. Seven (out of 16) unicoronal synostosis patients were selected, of whom four had Muenke syndrome, one had Saethre-Chotzen syndrome, and two had *TCF12*-related craniosynostosis. Of the 19 bicoronal synostosis patients, eight were selected, of whom six had Muenke syndrome, one had Saethre-Chotzen syndrome, and one had *TCF12*-related craniosynostosis.

The included 3D images were acquired from patients between the ages of 3.7 and 16.8 years.

The control group consisted of 89 children of the Generation-R study, Rotterdam, with a mean age of 10.8 years (SD 1.70). Twenty-four (out of 89) controls had 3D images taken at multiple timepoints, and were included in the longitudinal analysis.

3.2. Overall results

The pipeline developed by the authors was applied to the study

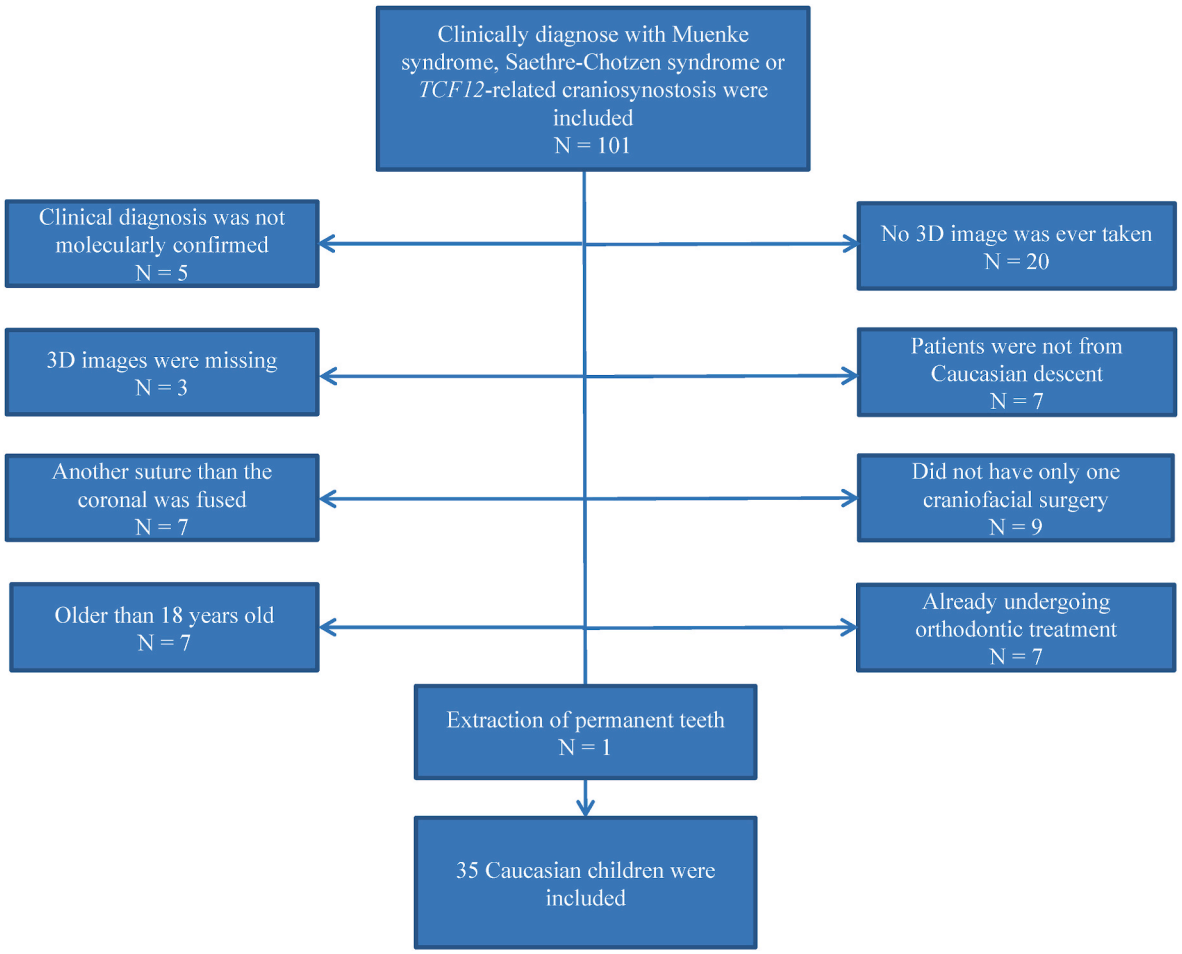

Fig. 2. Flowchart displaying the inclusion and exclusion criteria for patients and the final study group.

Table 1
Patient characteristics.

	Unicoronal, *N* = 16	Bicoronal, *N* = 19	Controls, *N* = 89
Males	*N* = 5	*N* = 6	*N* = 43
Females	*N* = 11	*N* = 13	*N* = 46
Mean age ±SD	11.0 ± 2.6	10.2 ± 3.6	10.8 ± 1.7
Muenke syndrome	*N* = 7	*N* = 11	
Saethre-Chotzen syndrome	*N* = 4	*N* = 4	
TCF12-related craniosynostosis	*N* = 5	*N* = 4	

population. Fig. 3 shows the output of facial heatmaps with MFA of selected examples of patients and controls. Notably, this figure illustrates how an increase in MFA corresponded with a higher degree of facial asymmetry.

3.3. Stratification analyses

Fig. 4 shows the MFA distribution of unicoronal and bicoronal synostosis patients and controls. Patients with unicoronal synostosis had an overall higher MFA than controls or patients with bicoronal synostosis.

Table 2 shows the MFA results for patients stratified according to three different syndromes. It shows that Muenke syndrome had an overall higher MFA than Saethre-Chotzen syndrome and *TCF12*-related craniosynostosis. Table 3 shows that MFA was higher in uni- and bicoronal synostosis compared with the controls after dividing the face into three facial segments. MFA decreased in severity from the upper part to the lower part of the face.

3.4. Longitudinal analysis

Fig. 5 shows the results of MFA in longitudinal analysis. The average slopes (MFA/year) were −0.003 (SD 0.016), 0.021 (SD 0.007), and 0.011 (SD 0.016) for controls, unicoronal synostosis, and bicoronal synostosis, respectively. MFA for the bicoronal synostosis patients and the controls showed a random pattern in follow-up. However, a trend of increasing MFA was seen in unicoronal synostosis patients.

4. Discussion

In this retrospective cross-sectional study, it was found that MFA in general was around two-to-three times higher in unicoronal synostosis patients, and about one-and-a-half times higher in bicoronal synostosis with Muenke syndrome, Saethre-Chotzen syndrome, and *TCF12*-related craniosynostosis compared with the control group. Asymmetry was most profound in Muenke syndrome patients.

MFA in patients with unicoronal craniosynostosis was, in general, around twice as high compared with MFA in patients with bicoronal craniosynostosis. Although both unicoronal and bicoronal patients had undergone only one craniofacial surgery, the difference in postsurgical MFA in unilateral synostosis and bilateral synostosis could be explained by an initially higher MFA presurgically in unilateral synostosis (Öwall et al., 2019). Moreover, children with bicoronal synostosis exhibited more facial asymmetry than anticipated, given the symmetrical nature of the condition. The authors hypothesize that this deviation could be

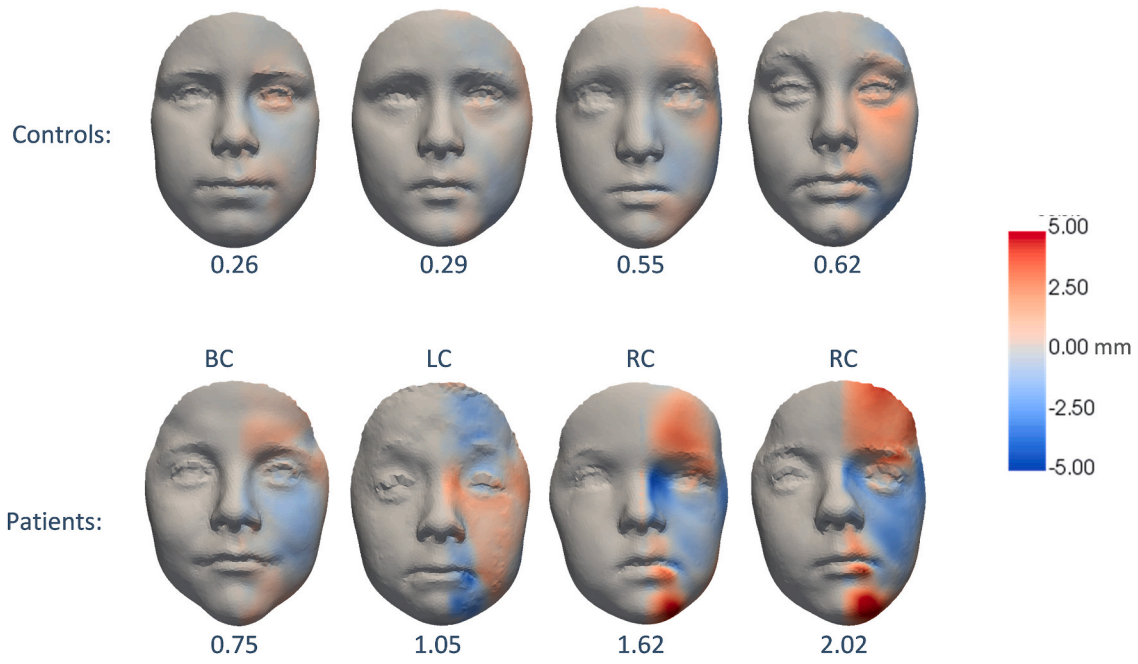

Fig. 3. Selected examples for controls and patients. Mean facial asymmetry is indicated below each face. BC: bicoronal synostosis; RC: right coronal synostosis; LC: left coronal synostosis. The colored half of the face represents asymmetrical features (red: expanding outward with respect to the contralateral half).

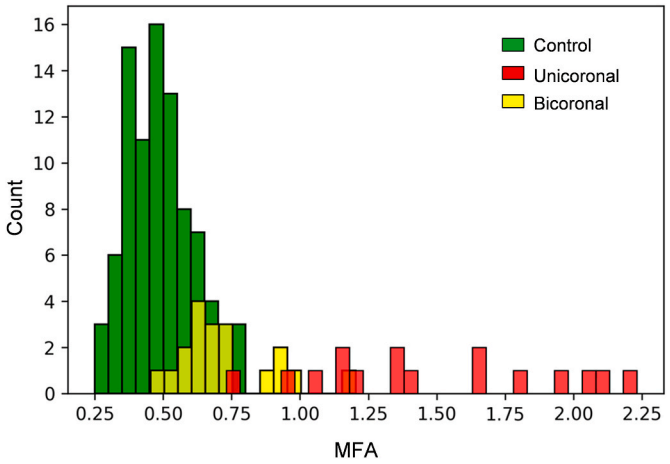

Fig. 4. Mean facial asymmetry (MFA) distribution for individual patients with unicoronal synostosis, bicoronal synostosis, and controls. Each bar represents one patient or control case.

Table 2
Mean facial asymmetry for different syndromes.

	Unicoronal	Bicoronal	Controls
Muenke syndrome	1.74 ± 0.40 mm ($N = 7$)	0.77 ± 0.21 mm ($N = 11$)	0.49 ± 0.12 mm ($N = 89$)
Saethre-Chotzen syndrome	1.15 ± 0.20 mm ($N = 4$)	0.69 ± 0.16 mm ($N = 4$)	
TCF12-related craniosynostosis	1.40 ± 0.51 mm ($N = 5$)	0.66 ± 0.05 mm ($N = 4$)	

attributed to craniofacial surgery not being completely symmetrical or varying closure times of the involved sutures, resulting in increased facial asymmetry in these syndromic children.

It was found that MFA was highest for the upper third of the face in unicoronal and bicoronal craniosynostosis patients with Muenke syndrome, Saethre-Chotzen syndrome, and *TCF12*-related craniosynostosis.

Table 3
Mean facial asymmetry in three facial segments.

	Unicoronal ($N = 16$)	*p*-value (unicoronal vs control)	Bicoronal ($N = 19$)	*p*-value (bicoronal vs control)	Controls ($N = 89$)
Upper face	1.95 ± 0.79 mm	$p < 1e\text{-}27$	0.88 ± 0.35 mm	$p < 1e\text{-}10$	0.49 ± 0.12
Mid face	1.44 ± 0.44 mm	$p < 1e\text{-}33$	0.77 ± 0.18 mm	$p < 1e\text{-}12$	0.50 ± 0.13
Lower face	1.31 ± 0.42 mm	$p < 1e\text{-}24$	0.62 ± 0.18 mm	$p < 1e\text{-}3$	0.49 ± 0.17

p-values are from linear regression, where the dependent variable was mean facial asymmetry, and the independent variable was with (1) or without (0) craniosynostosis; the covariates were age and sex. *p*-values were corrected for age and sex.

No clear patterns were seen in the longitudinal MFA data for the controls. Facial asymmetry may have increased or decreased during early puberty in the Dutch control group. These patterns of change in facial asymmetry over time have previously been reported in healthy children (Becker et al., 2006). The patients with bicoronal craniosynostosis displayed a similar pattern of change in facial asymmetry over time. A unique finding, however, was the steady increase in facial asymmetry over time exclusively in unicoronal craniosynostosis patients. Surgery itself may add to asymmetry, considering the asymmetry found in bicoronal synostosis patients in this study.

The method used in this study to objectify MFA took the presence of facial asymmetry in a healthy population into account. It is recognized that absolute facial symmetry is rare, and that a degree of facial asymmetry is commonly found in healthy individuals (Ekrami et al., 2020). The definition of facial asymmetry in patients in this study was based on the statistical significance of the deviation in their facial asymmetry compared with the controls.

Only three studies have examined the facial asymmetry in three dimensions using photogrammetry in patients with unicoronal craniosynostosis, and compared these with a control group. However, in these studies landmarks were placed manually, or asymmetry was determined manually, thereby increasing the influence of measurement error

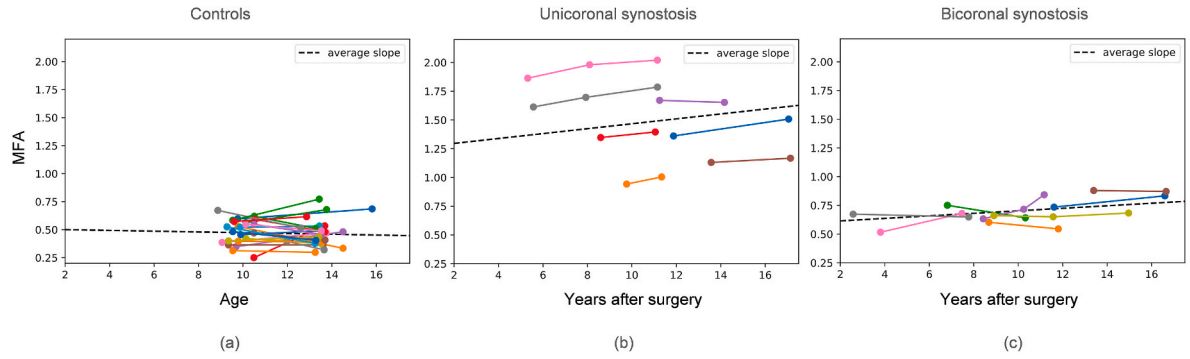

Fig. 5. Mean facial asymmetry at follow-up: a) controls; b) patients with unicoronal synostosis; c) patients with bicoronal synostosis. The dashed lines show the average slopes for the groups.

compared with the fully automated approach presented in our study (Cornelissen et al., 2013; Öwall et al., 2016, 2019). The presented approach therefore provides a more objective and reliable assessment of MFA.

Certain limitations that were acknowledged in this study included the small sample size after stratification of syndromic patients, which posed challenges for statistical analysis due to a lack of power. From a clinical point of view, the size of the syndromic group was significant considering the rarity of the disease, and provides clinicians with valuable insights into the differences in facial asymmetry between uni- and bicoronal synostosis patients and controls. Another limitation was the lack of preoperative 3D images of syndromic patients. Such images could aid in determining a preoperative facial asymmetry baseline and in quantifying the differences in MFA between syndromes before and after surgery, thereby enhancing the understanding of the effect of surgery on facial symmetry and its development over time. Lastly, another limitation was the smaller age range of the control group compared with that of the syndromic patients. Therefore, the development of MFA in controls younger than 9 years remains unknown.

Recently, 3D images have been acquired in all craniosynostosis patients shortly before and after craniofacial surgery within the Erasmus Medical Centre because the preoperative severity of craniofacial malformation may play an important role in the postoperative phenotype identified in this study. Moreover, surgery is not able to completely correct asymmetry in unicoronal craniosynostosis patients, in which asymmetry also increases over time. Future studies based on such data might help to understand the higher MFA values found in Muenke syndrome, and could provide critical insights into whether surgical planning for Muenke syndrome patients with unilateral synostosis should consider even more overcorrection than currently performed.

5. Conclusions

In this study, it was shown that the MFA was higher in unicoronal and bicoronal synostosis patients diagnosed with Muenke syndrome, Saethre-Chotzen syndrome, and *TCF12*-related craniosynostosis compared with healthy controls. In the syndromic group, the highest MFA was observed in patients with Muenke syndrome affected by unilateral synostosis.

Interestingly, syndromic children diagnosed with bicoronal synostosis exhibited more facial asymmetry than anticipated, given the symmetrical nature of the condition. The authors hypothesize that this deviation could be attributed to varying closure times of the involved sutures, resulting in increased facial asymmetry in these syndromic children.

Longitudinal analysis showed a seemingly random MFA pattern in bicoronal synostosis patients and controls, while an increasing MFA trend was observed in unicoronal synostosis patients.

The authors advocate for use of the presented automated framework for quantitative analysis of facial asymmetry, coupled with the continual advancement of quantitative methodologies designed for 3D data. This will facilitate more objective studies and contribute to improved surgical results in the future.

Funding

This research did not receive any specific grant from funding agencies in the public, commercial, or not-for-profit sectors.

References

Alabort-i-Medina, J., Antonakos, E., Booth, J., Snape, P., Zafeiriou, S., Menpo, 2014. A comprehensive platform for parametric image alignment and visual deformable models. MM'14: Proc. 22nd ACM Int. Conf. Multimedia 679–682. https://doi.org/10.1145/2647868.2654890.

Becker, D.B., Fundakowski, C.E., Govier, D.P., Deleon, V.B., Marsh, J.L., Kane, A.A., 2006. Long-term osseous morphologic outcome of surgically treated unilateral coronal craniosynostosis. Plast. Reconstr. Surg. 117, 929–935. https://doi.org/10.1097/01.prs.0000200613.06035.51.

Bellus, G.A., Gaudenz, K., Zackai, E.H., Clarke, L.A., Szabo, J., Francomano, C.A., Muenke, M., 1996. Identical mutations in three different fibroblast growth factor receptor genes in autosomal dominant craniosynostosis syndromes. Nat. Genet. 14, 174–176. https://doi.org/10.1038/ng1096-174.

Booth, J., Roussos, A., Ponniah, A., Dunaway, D., Zafeiriou, S., 2018. Large scale 3D morphable models. Int. J. Comput. Vis. 126, 233–254. https://doi.org/10.1007/s11263-017-1009-7.

Chotzen, F., 1932. Eine eigenartige familiaere Entwicklungsstoerung (Akrocephalosyndaktylie, Dysostosis craniofacialis und Hypertelorismus). Monatsschr. Kinderheilkd. 55, 97–122.

Cornelissen, M.J., van der Vlugt, J.J., Willemsen, J.C.N., van Adrichem, L.N.A., Mathijssen, I.M.J., van der Meulen, J.J.N.M., 2013. Unilateral versus bilateral correction of unicoronal craniosynostosis: an analysis of long-term results. J. Plast. Reconstr. Aesthetic Surg. 66, 704–711. https://doi.org/10.1016/j.bjps.2013.01.033.

Cornelissen, M., den Ottelander, B., Rizopoulos, D., van der Hulst, R., Mink van der Molen, A., van der Horst, C., Delye, H., van Veelen, M., Bonsel, G., Mathijssen, G., 2016. Increase of prevalence of craniosynostosis. J. Cranio-Maxillo-Fac. Surg. 44, 1273–1279. https://doi.org/10.1016/j.jcms.2016.07.007.

De Goederen, R., Yang, S., Pullens, B., Wolvius, E.B., Joosten, K.F.M., Mathijssen, I.M.J., 2021. Evaluation of the OSA treatment protocol in syndromic craniosynostosis during the first 6 years of life. J. Plast. Reconstr. Aesthetic Surg. 74, 2674–2682. https://doi.org/10.1016/j.bjps.2021.03.033.

Den Ottelander, B.K., de Goederen, R., van Veelen, M.L.C., van de Beeten, S.D.C., Lequin, M.H., Dremmen, M.H.G., Loudon, S.E., Telleman, M.A.J., de Gier, H.H.W., Wolvius, E.B., Tjoa, S.T.H., Versnel, S.L., Joosten, K.F.M., Mathijssen, I.M.J., 2019. Muenke syndrome: long-term outcome of a syndrome-specific treatment protocol. J. Neurosurg. Pediatr. 19, 1–8. https://doi.org/10.3171/2019.5.PEDS1969.

Doherty, E.S., Lacbawan, F., Hadley, D.W., Brewer, C., Zalewski, C., Jeff Kim, H., Solomon, B., Rosenbaum, K., Domingo, D.L., Hart, T.C., Brooks, B.P., Immken, L., Brian Lowry, R., Kimonis, V., Shanske, A.L., Jehee, F.S., Bueno, M.R.P., Knightly, C., McDonald-McGinn, D., Zackai, E., Muenke, M., 2007. Muenke syndrome (FGFR3-related craniosynostosis): expansion of the phenotype and review of the literature. Am. J. Med. Genet. 15, 3204–3215. https://doi.org/10.1002/ajmg.a.32078.

Ekrami, O., Claes, P., White, J.D., Weinberg, S.M., Marazita, M.L., Walsh, S., Shriver, M., 2020. A multivariate approach to determine the dimensionality of human facial asymmetry. Symmetry (Basel) 12, 348. https://doi.org/10.3390/sym12030348.

El Ghouzzi, V., Le Merrer, M., Perrin-Schmitt, F., Lajeunie, E., Benit, P., Renier, D., Bourgeois, P., Bolcato-Bellemin, A.L., Munnich, A., Bonaventure, J., 1997. Mutations of the TWIST gene in the Saethre-Chotzen syndrome. Nat. Genet. 15, 42–46. https://doi.org/10.1038/ng0197-42.

El Ghouzzi, V., Lajeunie, E., Le Merrer, M., Cormier-Daire, V., Renier, D., Munnich, A., Bonaventure, J., 1999. Mutations within or upstream of the basic helix-loop-helix domain of the TWIST gene are specific to Saethre-Chotzen syndrome. Eur. J. Hum. Genet. 7, 27–33. https://doi.org/10.1038/sj.ejhg.5200240.

Ercan, I., Ozdemir, S.T., Etoz, A., Sigirli, D., Shane Tubbs, R., Loukas, M., Guney, I., 2008. Facial asymmetry in young healthy subjects evaluated by statistical shape analysis. J. Anat. 213, 663–669. https://doi.org/10.1111/j.1469-7580.2008.01002.x.

Ferrario, V.F., Sforza, C., Pizzini, G., 1993. Sexual dimorphism in the human face assessed by Euclidean distance matrix analysis. J. Anat. 183, 593–600.

Gallagher, E.R., Ratisoontorn, C., Cunningham, M.L., 2003. Saethre-Chotzen syndrome. In: Adam, M.P., Mirzaa, G.M., Pagon, R.A., et al. (Eds.), GeneReviews® [Internet]. University of Washington, Seattle, Seattle (WA), pp. 1993–2023 [Updated 2019 Jan 24].

Hohoff, A., Joos, U., Meyer, U., Ehmer, U., Stamm, T., 2007. The spectrum of Apert syndrome: phenotype, particularities in orthodontic treatment, and characteristics of orthognathic surgery. Head Face Med. 8, 10. https://doi.org/10.1186/1746-160X-3-10.

Howard, T.D., Paznekas, W.A., Green, E.D., Chiang, L.C., Ma, N., Ortiz De Luna, R.I., Garcia Delgado, C., Gonzalez-Ramos, M., Kline, A.D., Jabs, E.W., 1997. Mutations in TWIST, a basic helix-loop-helix transcription factor, in Saethre-Chotzen syndrome. Nat. Genet. 15, 36–41. https://doi.org/10.1038/ng0197-36.

Jaddoe, V.W.V., Mackenbach, J.P., Moll, H.A., Steegers, E.A.P., Tiemeier, H., Verhulst, F. C., Witteman, J.C.M., Hofman, A., 2006. The Generation R Study: design and cohort profile. Eur. J. Epidemiol. 21, 475–484. https://doi.org/10.1007/s10654-006-9022-0.

Muenke, M., Gripp, K.W., McDonald-McGinn, D.M., Gaudenz, K., Whitaker, L.A., Bartlett, S.P., Markowitz, R.I., Robin, N.H., Nwokoro, N., Mulvihill, J.J., Losken, H. W., Mulliken, J.B., Guttmacher, A.E., Wilroy, R.S., Clarke, L.A., Hollway, G., Adès, L. C., Haan, E.A., Mulley, J.C., Cohen Jr., M.M., Bellus, G.A., Francomano, C.A., Moloney, D.M., Wall, S.A., Wilkie, A.O., Zackai, E.H., 1997. A unique point mutation in the fibroblast growth factor receptor 3 gene (FGFR3) defines a new craniosynostosis syndrome. Am. J. Hum. Genet. 60, 555–564.

Öwall, L., Darvann, T.A., Larsen, P., Hove, H.D., Hermann, N.V., Bøgeskov, L., Kreiborg, S., 2016. Facial asymmetry in children with unicoronal synostosis who have undergone craniofacial reconstruction in infancy. Cleft Palate Craniofac. J. 53, 385–393. https://doi.org/10.1597/15-089.

Öwall, L., Darvann, T.A., Hove, H.B., Bøgeskov, L., Kreiborg, S., Hermann, N.V., 2019. Spatially detailed 3D quantification of improved facial symmetry after surgery in children with unicoronal synostosis. Cleft Palate Craniofac. J. 56, 918–928. https://doi.org/10.1177/1055665618821821.

Saethre, M., 1931. Ein Beitrag zum Turmschaedelproblem (Pathogenese, Erblichkeit und Symptomatologie). Dtsch. Z. für Nervenheilkd. 119, 533–555.

Seabold, S., Perktold, J., Statsmodels, 2010. Econometric and statistical modeling with python. Proc. 9th Python Sci. Conf. 57–61. https://doi.org/10.25080/Majora-92bf1922-011.

Virchow, R., 1851. Über den Cretinismus, namentlich in Franken, und über pathologische Schädelformen. Verb Phys. Med. Ges. 2, 230–256.

Web references

LightOfMonet https://github.com/LightOfMonet/3Dface_landmark, accessed July 26, 2023.

pcregistericp https://nl.mathworks.com/help/vision/ref/pcregistericp.html, accessed January 3, 2023.